SOLAR POWER PLANT IN A MODERN OFFICE BUILDING: POWER AND POWER QUALITY CONSIDERATIONS

Antti HILDEN
Tampere University
Finland
antti.t.hilden@tuni.fi

Pertti PAKONEN
Tampere University
Finland
pertti.pakonen@tuni.fi

Pekka VERHO
Tampere University
Finland
pekka.verho@tuni.fi

ABSTRACT

The increasing usage of power electronic devices and changes in time domain characteristics of power generation and electricity markets motivate the studies of this paper. The electrical energy system of a modern office building is comprehensively monitored with advanced power meters and the influence of solar power plant and various load types is examined on power flows and voltage and current distortion. The study presents the behavior of active and reactive power with several time averages considering separately measured loads and solar power plant. In addition, Fryze's power theory is discussed with the aid of total distortion measurements. The results offer an overview of the effect of time averaging on power measurements and a case study, in which distortion is included in power quantity.

INTRODUCTION

The challenges of distribution networks in the future involve larger and more rapid fluctuations in power flows and increasing amount of voltage distortion [1]. The development towards "smart grid" concept and the will to produce renewable energy have introduced non-dispatchable distributed generation (DG) and commissioning of demand side management (DSM) that affect the magnitude and direction of power flows. Additionally, the European day-ahead electricity market is shifting its imbalance settlement period (ISP) from 1 hour to 15 minutes by 1st of January 2025 at latest and power tariffs are emerging even for smaller customers. At the same time, the utilization of power electronics is growing in consumer devices, e.g. solar inverters, electric car chargers and lighting. These devices are nonlinear and electronically coupled, and thus generate current distortion at various frequencies and eventually distort voltage.

It is obvious that more and more intermittent DG will be connected to distribution networks in the upcoming years. Therefore, the feasible time resolution of power measurements needs to be determined considering the behavior of power flows and electricity markets. The proliferation of modern power electronic devices encourages examination of power theories differing from the conventionally used. An appropriate power quantity can measure voltage and current distortion disturbances induced by distribution network customers, and thus the responsibility of the disturbances is shared between distribution network operator (DSO) and its customers. In adverse situations, distortion in voltage or current overloads transformer and causes malfunctions in devices and resonances in distribution network. These result in costs for the DSO and the customers. On the other hand, a power quantity involving distortion can be utilized when the efficiency of the distribution network is assessed and the sources of voltage distortion are traced.

This paper approaches the issues from the viewpoint of measurements in real environment of a modern office building. The electrical behavior of a solar power plant is compared to loads including ventilation and cooling. The focus of the paper is on time averaging of power and distortion in current and power.

POWER THEORY AND DISTORTION

Electrical power is frequently divided into active and reactive power in brevity of common conversations. However, depending on the calculation method or power theory especially the magnitude of reactive power may vary drastically. This paper concerns measuring of active, fundamental frequency reactive and Fryze's reactive power using phase-to-neutral measurements in low voltage distribution network. Phase-to-neutral measurements were chosen to produce explicit results and avoid the complexities of three-phase quantities. Furthermore, large portion of customer devices is connected between the phase and neutral conductor and power quality standards, e.g. EN 50160, define the limits for phase-to-neutral values.

Numerous power theories exist in the literature. However, apparent power of one phase is in general calculated as the product of phase voltage and current as in Equation 1.

$$S = UI \ \left[\mathrm{VA}\right] \tag{1}$$

The root mean square (rms) of voltage and current are denoted with U and I, respectively. Apparent power presents the maximum power, at which net energy can be delivered in an ideal case. Conventionally S is presented to consist of fundamental frequency active (P_1) and reactive power (Q_1) shown in Equation 2. However, this is true only in sinusoidal conditions of distribution network when no distortion is measured in voltage or current.

$$S = \sqrt{P_1^2 + Q_1^2} \ \left[\mathrm{VA}\right] \tag{2}$$

Power theory developed by Fryze constitutes a simple aspect for power measurements. Fryze divides current to two orthogonal components, active and reactive current, hence S includes active power (P) and Fryze's reactive power (Q_f). These power components contain also the distortion components of voltage and current. The calculation of Fryze's reactive power is derived in Equation 3. [2] Q_f is equivalent to nonactive power defined in standard IEEE Std 1459.

$$Q_f = \sqrt{S^2 - P^2} \ \left[\text{VAr}\right] \tag{3}$$

Both Q_1 and reactive distortion power are included in Q_f, therefore the magnitude of Q_1 remains unknown without an additional measurement. Nevertheless, both Q_1 and reactive distortion power are usually undesirable for DSOs and could be incorporated in the same quantity. The distortion part of Q_f comprises voltage and current components that deviate from the sinusoidal waveform. This paper considers harmonic, interharmonic and subharmonic components in the bandwidth of 0-2 kHz enabled by the design of the meter used. Also standard EN 50160 considers harmonics until 2 kHz.

Differing from commonly used total harmonic distortion (THD) this paper defines the measurements of distortion with total distortion (TD) that is described in Equation 4 in simplified form. Contrary to integer harmonics in THD, TD involves every frequency component of distortion of a waveform omitting DC-component, and therefore also the amount of subharmonics and interharmonics is quantified.

$$TD_I = \frac{I_{TD}}{I_1} \times 100 \ \left[\%\right] \tag{4}$$

Total distortion of current, TD_I, is expressed as percentage from the ratio of rms total distortion current, I_{TD}, and rms fundamental frequency current, I_1. Basically I_{TD} is the remaining rms current after subtracting I_1 and DC-component from the total current measured in the frequency range of 0-2 kHz. The value of I_{TD} is averaged over time conforming with standard IEC 61000-4-30. In the study, I_{TD} is extracted from Equation 4 by cancelling I_1 as deduced in Equation 5. This was possible because the measurements included I_1. Equations 4 and 5 also apply for distortion voltage (TD_U and U_{TD}).

$$I_{TD} = \frac{I_{TD}}{I_1} I_1 \times 0.01 = TD_I I_1 \times 0.01 \ \left[\text{A}\right] \tag{5}$$

Contrary to fundamental frequency magnitude relative THD and TD, the value of I_{TD} can be used to compare the distortions of measurements in absolute manner. In low load conditions THD may express overly high and misleading values when the magnitude of the fundamental frequency component is small. This is especially the case with solar power plants as e.g. Pakonen et al. report [3].

PILOT BUILDING AND MEASUREMENTS

The measurements of the paper are performed in an eight-storey modern multi-user office building located at Tampere University in Finland. The building is called Kampusareena and was completed in 2015. Kampusareena offers facilities for the offices of companies, commercial premises, e.g. restaurants, and university premises including library and studying areas. Photograph of the building is shown in Figure 1.

Figure 1. *Photograph of the pilot building Kampusareena.*

A pilot system was implemented on Kampusareena, which enabled a complete monitoring of the electrical energy system with advanced power meters. Additionally, the data of solar inverters, building automation, weather station and forecast, electricity market price and the national transmission network status was gathered with the same ICT system that monitors the building. [4]

The electrical loads that are monitored separately include ventilation, two cooling units, two elevators and electric car charging station. In addition, solar power plant and the aggregation of two main distribution boards and access point to medium voltage distribution network are measured. The loads and solar power plant are specified in detail in the thesis [4]. Solar power plant supplies ventilation in parallel with the main distribution board. Other groups of service electricity contain negligibly small appliances in terms of power. The loads of tenants' electricity consist of e.g. lighting and appliances plugged into wall sockets but they are left without further separation. The main electricity distribution and measured loads are depicted in Figure 2, in which meter locations are denoted with M. The building uses district heating.

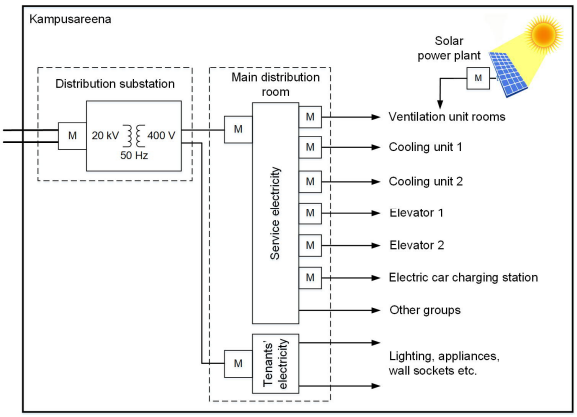

Figure 2. *Main electricity distribution system of Kampusareena.*

The measurements of the electrical energy system are recorded as 1 second averages for a wide range of voltage, current, power and other electrical quantities. The meters have bandwidth of 0-2 kHz and they monitor all three phases of the system. The measurement data has been collected for several months and the pilot is continuing in year 2019. The diverse features of the pilot environment allow various other examinations in the future.

TIME AVERAGING OF POWER

The time domain behavior analysis of the paper utilized the time resolution of 1 second of the measurements. Averages of 1 minute, 5 minutes, 15 minutes and 1 hour were computed for active power (P), fundamental frequency reactive power (Q_1) and Fryze's reactive power (Q_f). The power averages were studied in cases of the different load types and the solar power plant. The calculated averages are arithmetic means based on the measured 1 second averages. Time average of power is frequently also called as average demand.

Only elevator 1 and cooling unit 2 were selected in the study because the elevators and the cooling units behave similarly to each other. The chosen elevator and cooling unit presented the highest activity in terms of active power during the observed day. The measurements of the main distribution boards are omitted to concentrate on the individual loads. The effect of time averaging is exemplified in Figure 3, in which 1 minute, 15 minutes and 1 hour averages are illustrated in time domain. The examinations use the measurements of phase 1 (L1) throughout the paper as explained in the theory section.

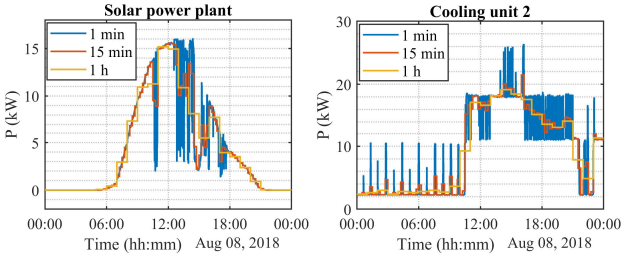

Figure 3. *Time averaging examples of active power (P) in cases of solar power plant and cooling unit 2.*

Fluctuations of P can be observed in Figure 3 with different time averages. It is notable that especially 1 minute average deviates largely from 1 hour and 15 minutes averages at the measurement points. The characteristics of the calculated time averages were also investigated by means of cumulative distribution functions (cdf) as depicted in Figure 4. The results of cdf reveal the probability for a range of active power magnitudes on 8th of August 2018. The characteristics of the cdf computations of P, Q_1 and Q_f are listed in Tables 1-3, in addition to other statistics of the time averages. Negative Q_1 represents capacitive and positive Q_1 inductive reactive power. The sign of P of solar power plant is inverted to present positive magnitudes.

In Figure 4, the cdf curves demonstrate how the distributions of the different time averages conform with each other. Except for elevator 1, the cdf curves of 1 second and 1 minute are nearly equal, hence 1 minute average can sufficiently give information from the time domain behavior of P in the pilot building. At the same time, average of 1 hour differentiates remarkably from all the other averages, and thus conceals power fluctuations. Also Wright has reported similar result to this paper [5]. Observing of cloudy days revealed that without the connection to solar power plant the average of 1 hour of ventilation would follow the 1 second curve. The knowledge about time variations of power can be useful, if for example a management of power flow is designed or the influence of a power tariff or a shorter time period electrical energy market is investigated.

The characteristics in Tables 1-3 contain five columns named as *median*, *min*, *max*, *1 h min* and *1 h max*. The value of *median* is the middlemost value when the values are sorted by magnitude. *min* and *max* represent the smallest and highest magnitudes of the averaged values, and lastly *1 h min* and *1 h max* list the probability of cdf at *min* and *max* magnitudes of 1 hour average, at which 1 hour has respectively either 0 % or 100 % probability.

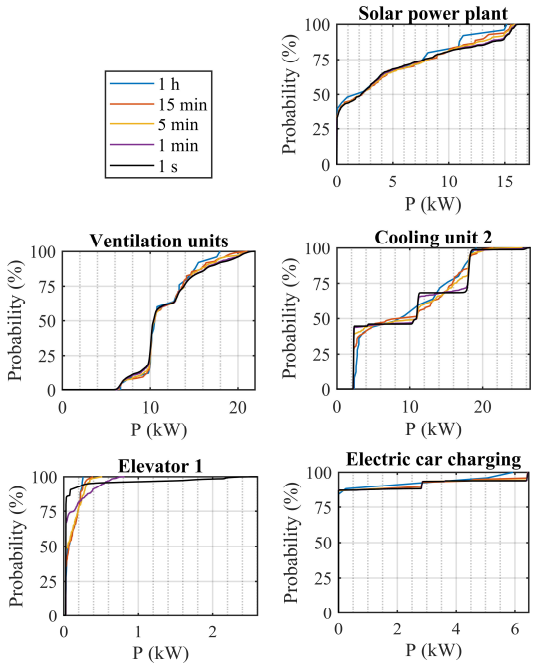

Figure 4. *Cumulative distribution functions of time averages of active power (P) for solar power plant and loads on 8th of August 2018.*

The characteristics in the tables show congruently that the averaging barely affects *median* but *min* and *max* change toward smaller and higher magnitude respectively as the averaging period shortens. In a few occasions, 1 second average of *min* or *max* remarkably differs from the other averages due to a some transient in the measurement. Generally the average of 15 minutes, 5 minutes or 1 minute

already nearly reaches the same *min* or *max* magnitude as 1 second, while the characteristics of 1 hour express a large difference to the other time averages.

Table 1. *Characteristics of time averages of P for solar power plant and loads on 8th of August 2018.*

		Median [kW]	Min [kW]	Max [kW]	1 h min [%]	1 h max [%]
Solar power plant	1 h	2.4	0.0	15.2	0	100
	15 min	2.3	0.0	15.5	10	96
	5 min	2.2	0.0	15.9	10	95
	1 min	2.2	0.0	16.1	9	93
	1 s	2.2	0.0	17.2	11	92
Ventilation units	1 h	10.6	6.6	17.9	0	100
	15 min	10.5	6.5	21.0	3	96
	5 min	10.5	6.4	21.3	4	95
	1 min	10.4	6.1	21.6	4	93
	1 s	10.4	0.0	22.0	4	92
Cooling unit 2	1 h	9.3	2.4	19.2	0	100
	15 min	11.0	2.3	21.5	30	96
	5 min	11.0	2.3	25.5	39	97
	1 min	10.9	2.3	26.4	43	98
	1 s	10.9	0.0	26.5	44	99
Elevator 1	1 h	0.1	0.0	0.3	0	100
	15 min	0.1	0.0	0.4	18	95
	5 min	0.1	0.0	0.5	23	87
	1 min	0.0	0.0	0.8	30	84
	1 s	0.0	0.0	2.6	36	94
Electric car charging	1 h	0.0	0.0	5.9	0	100
	15 min	0.0	0.0	6.4	0	96
	5 min	0.0	0.0	6.4	0	94
	1 min	0.0	0.0	6.5	0	94
	1 s	0.0	0.0	6.5	0	94

Table 2. *Characteristics of time averages of Q_1 for solar power plant and loads on 8th of August 2018.*

		Median [kVAr]	Min [kVAr]	Max [kVAr]	1 h min [%]	1 h max [%]
Solar power plant	1 h	-0.1	-0.1	0.1	0	100
	15 min	-0.1	-0.1	0.1	5	96
	5 min	-0.1	-0.1	0.1	6	96
	1 min	-0.1	-0.2	0.1	7	96
	1 s	-0.1	-0.9	0.8	9	95
Ventilation units	1 h	-0.1	-2.3	1.6	0	100
	15 min	-0.1	-2.5	1.8	3	98
	5 min	-0.1	-2.6	1.8	4	96
	1 min	-0.1	-2.9	2.0	4	96
	1 s	-0.1	-3.1	2.7	5	95
Cooling unit 2	1 h	5.1	-0.3	13.0	0	100
	15 min	6.7	-0.5	14.7	30	97
	5 min	6.7	-0.5	17.2	38	97
	1 min	6.7	-0.5	18.0	42	98
	1 s	6.7	-0.6	19.5	40	98
Elevator 1	1 h	-0.1	-0.1	-0.1	0	100
	15 min	-0.1	-0.1	0.0	6	95
	5 min	-0.1	-0.1	0.0	9	90
	1 min	-0.1	-0.1	0.0	21	86
	1 s	-0.1	-0.3	0.5	28	95
Electric car charging	1 h	0.0	-0.2	0.0	0	100
	15 min	0.0	-0.2	0.0	6	100
	5 min	0.0	-0.2	0.0	6	100
	1 min	0.0	-0.2	0.0	6	100
	1 s	0.0	-0.6	0.5	6	100

Table 3. *Characteristics of time averages of Q_f for solar power plant and loads on 8th of August 2018.*

		Median [kVAr]	Min [kVAr]	Max [kVAr]	1 h min [%]	1 h max [%]
Solar power plant	1 h	0.5	0.1	1.4	0	100
	15 min	0.5	0.1	1.4	5	97
	5 min	0.5	0.1	1.4	6	95
	1 min	0.5	0.0	1.4	7	92
	1 s	0.5	0.0	5.4	4	91
Ventilation units	1 h	11.1	6.9	15.2	0	100
	15 min	11.3	6.8	15.2	5	99
	5 min	11.4	6.8	15.3	8	98
	1 min	11.4	5.7	15.4	7	97
	1 s	11.4	0.0	19.1	6	97
Cooling unit 2	1 h	7.2	3.7	13.4	0	100
	15 min	7.6	3.2	15.1	19	97
	5 min	7.6	3.2	17.6	21	97
	1 min	7.5	3.2	18.3	23	98
	1 s	7.5	0.0	44.5	23	98
Elevator 1	1 h	0.1	0.1	0.2	0	100
	15 min	0.1	0.1	0.3	15	93
	5 min	0.1	0.1	0.3	19	86
	1 min	0.1	0.1	0.4	18	83
	1 s	0.1	0.0	1.6	17	92
Electric car charging	1 h	0.0	0.0	0.4	0	100
	15 min	0.0	0.0	0.4	0	96
	5 min	0.0	0.0	0.4	0	94
	1 min	0.0	0.0	0.4	0	94
	1 s	0.0	0.0	1.8	0	94

The percentage of *1 h min* increases as the time averaging period decreases and *1 h max* decreases in similar manner in general. However, inconsistencies are found because of the intersecting shapes of the cdf curves as can be observed from Figure 4. The characteristics of the tables offer case results considering the influence of time averaging on *P* and Q_1 and the effect of distortion power in Q_f.

DISTORTION IN VOLTAGE, CURRENT AND POWER

The measurements of the pilot building enabled to study the correlation of Q_f to current (I_{TD}) and voltage distortion (U_{TD}) and the relation of Q_1 and *P* to Q_f during the same observation period. Additionally, it is possible to contrast the behavior of the load types and the solar power plant.

The same day as in the time averaging calculations is considered in Figure 5, which also contains cooling unit 1, elevator 2 and tenants' electricity. Except for Q_1 and U_{TD}, the measurements are stacked on each other meaning only tenants' electricity has reference point at zero of the y-axes. The stacked plotting style was chosen to visualize the comparison between the magnitudes of the loads and the solar power plant. Because most of the meters are positioned in the main distribution room, U_{TD} of service electricity main distribution board is used in the distortion voltage inspection.

Ventilation, that utilizes numerous frequency converters, with tenants' electricity, that is a blend of lighting and

other appliances, produce the highest Q_f. Also the cooling units generate notable amount of Q_f in addition to having largely inductive Q_1 because they utilize directly coupled compressors. The powers of the elevators and electric car charging are minimal compared with the other measurements, as in Tables 1-3. For the solar power plant, small Q_f, I_{TD} and Q_1 are measured, even though its active power equals to the cooling and ventilation during working hours. Although the daily variation of TD_I is large, I_{TD} is quite constant throughout the day [4]. The value of I_{TD} is the main cause for distortion part in Q_f due to relatively low U_{TD}. Overall, the magnitudes of Q_f remarkably differ from Q_1 while I_{TD} resembles Q_f by visual inspection. This indicates that the most part of distortion power is quantified with Q_f. Additionally, P correlates with Q_f and I_{TD}, hence distortion is dependent on active power.

CONCLUSION

As distribution networks are evidently changing due to renewable and distributed power generation and power electronic devices, it is reasonable to reconsider the quantification of power for the future power systems. This paper utilized the implemented monitoring system of the pilot building to study power quantities of solar power plant and loads of various types.

Active, fundamental frequency reactive and Fryze's reactive power were compared using several different time averages and cumulative distribution functions. The study listed the influence of the each time average and concluded that 1 hour average distinctly differs from the other averages. However, neither 1 second average is required unless the most rapid power peaks are under concern. Fryze's reactive power was examined because of its simple nature and growing distortion in voltage and current in distribution networks. The measurements revealed that distortion current is a dominant cause of distortion power and distortion is majorly reactive, hence quantified with Fryze's reactive power. Power electronics based tenants' electricity and ventilation were the major sources of Fryze's reactive power and the solar power plant and electric car charging induced minor effect to the system. However, aggregated effect of several devices or weaker network can worsen the situation. Finally, fundamental frequency reactive power was noted to remarkably deviate from Fryze's reactive power and distortion correlated noticeably with the magnitude of active power.

ACKNOWLEDGMENTS

Kampusareena pilot was implemented in cooperation with the companies participating in the project Social Energy – Prosumer Centric Energy Ecosystem (ProCem).

REFERENCES

[1] F. Zavoda et al., 2016, "Power quality in the future grid - Results from CIGRE/CIRED JWG C4.24", *17th International Conference on Harmonics and Quality of Power*, 931–936.

[2] L. S. Czarnecki, 1997, "Budeanu and Fryze: Two frameworks for interpreting power properties of circuits with nonsinusoidal voltages and currents", *Electr. Eng.*, vol. 80, 359–367.

[3] P. Pakonen et al., 2016, "Grid-connected PV power plant induced power quality problems - Experimental evidence", *18th European Conference on Power Electronics and Applications*, 1–10.

[4] A. Hilden, 2018, *Power quality and power monitoring in a modern office building utilizing diverse metering*, Master of Science Thesis, Tampere University of Technology.

[5] A. Wright et al., 2007, "The nature of domestic electricity-loads and effects of time averaging on statistics and on-site generation calculations", *Appl. Energy*, vol. 84, 389–403.

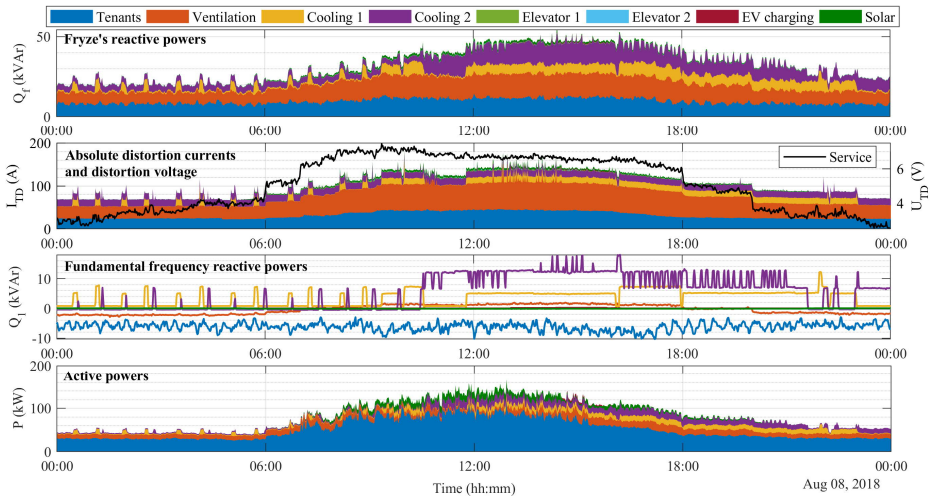

Figure 5. *Fryze's reactive power (Q_f), total distortion current (I_{TD}) and voltage (U_{TD}), fundamental frequency reactive power (Q_1) and active power (P) of solar power plant and loads in 1 second averages on 8th of August.*